Algerian Journal of Environmental Science and Technology
June edition. Vol.7. Nº2. (2021)
ISSN : 2437-1114
www.aljest.org

Performance analysis and optimization of molten a salt cavity receiver in solar power plants

A. Rouibah [1*], D. Benazzouz [1] , K. Rahmani[2], T. Benmessaoud[3]

[1] Mechanics Laboratory of Systems and Solids, Faculty of Engineering Sciences (FSI),M'Hamed Bougara University, Boumerdès 35000, Algeria
[2] Department of Engineering, University of Bab Ezzouar, Algiers 16311, Algeria
[3] Ingenium Group; University of Castilla La Mancha, Ciudad Real 13071, Spain

[*]Corresponding Author Email: a.rouibah@univ-boumerdes.dz ; rouibah_a@yahoo.fr ; Tel.: +213 5 50 6354 82

ARTICLE INFO

Article History :

Received ***:03/02/2020***
Accepted ***:11/07/2020***

***Key Words*:**

Clean energies; Energy balance; Genetic algorithms; Heat flux; Optimal efficiency; Performances; Power cycle; Solar tower concentrator.

ABSTRACT

Abstract: *The objective of this paper focuses on optimizing the performance of solar systems. These systems play an essential role in the production of electricity worldwide. They are sources of clean energy which can be exploited in areas rich with solar potential.*
In this paper, the goal is to optimize the heat flow absorbed by the receiver. To do this, genetic algorithms are proposed as an approach able of solving the problematic subject with constraints that are countable and interlinked. These constraints are inspired from the energy balance of the solar tower concentrator under study.
The results obtained by numerical analysis based on these constraints and the objective functions (maximizing the heat flow received and minimizing the losses of the heat flow) shows the existence of an optimal receiver efficiency value for the heliostat surface total, the receiver temperature, the molten salt temperature, the receiver opening surface, the receiver surface, the diameter, the thickness, the tubes thermal conductivity of the receiver and the steam flow at turbine inlet. In addition, the energy efficiency of the solar tower system improves better depending on the power cycle chosen such as the Hirn cycle with reheating and racking used in our case.

I. Introduction

Current electricity production does not meet the needs of the world because of the evolution of populations and the industrial revolution. This production is the source of fossil fuels such as petroleum, natural gas and coal. These traditional sources are polluting and exhausting, causing carbon dioxide emissions and global warming [1].
This is why, it is necessary to substitute these energies by other alternative and sustainable sources suitable for the production of electricity and which preserves the environment. One of these sources is solar energy which solar concentrators are the most exploited for their efficiency which are much better compared to other solar systems [2].
Thermodynamic solar or tower solar concentrating systems (CSP) is a technology that produces electricity by concentrating solar energy at a focal point using optical concentrator systems coupled to receiving systems. As all industrial equipment, CSP systems need to optimize their performance in order to improve their electricity production [2].
Several researches are carried out with the aim of improving the energy parameters of solar concentration systems (CSP), hence the optimization of their performance.
K. Wang et al. [3] . have developed an integrated model for the integrated SPT system including the heliostat field, the molten salt solar receiver, the thermal storage of molten salt and the Brayton cycle of S-CO_2 recompression with reheating.
Z. Liao et al [4] presented a new central solar heat pipe receiver for a molten salt solar energy tower. Composed of a reflector, a heat pipe and a receiver tube. The numerical simulation of the receiver gives impressive results, that to reach an efficiency of 91.5%.

Copyright © 2021, Algerian Journal of Environmental Science and Technology, All rights reserved

SSM.Tehrani et al. [5] have developed a validated thermal model which is suitable for design / non-design performance analyzes of receivers with molten salt cavities in steady state and in transient regime. The study examined two control strategies - a fixed receiver flow (FF) and a fixed receiver exit temperature (FT) - for their off-design performance in each of the two off-design operating modes (storage and non-storage) .

S. Benammar et al. [6] proposed a mathematical model developed based on energy analysis for the simulation of the performance of solar tower power plants (STPP) without energy storage. A general nonlinear mathematical model of the studied system (STPP) has been presented and solved using numerical optimization methods.

Chao Xu et al. [7] presented a theoretical study for the energy and exergy analysis of the solar energy tower system using molten salt as heat transfer fluid. Several design parameters, including direct normal irradiation (DNI), concentration ratio and power cycle type are tested to evaluate their effects on energy and exergy performance.

Yao et al. [8] modeled and simulated the pioneering 1 MW solar thermal central receiver (CRS) system in China (DAHAN). Based on the energy balance, they developed the mathematical models of the main basic components in the CRS and integrated them into a whole plant model.

Prakash et al. [9] conducted an experimental and numerical study of steady-state convective heat loss from a down-facing cylindrical cavity receiver.

Montes et al. [10,11] studied the influence of the solar multiple on the annual performance of parabolic trough solar power plants with direct steam generation. Thermal analysis and economic analysis were done in their work.

Larbi et al. [12] presented the performance analysis of a stack solar plant based on energy balance, and also studied the effects of various factors on thermal performance, including solar radiation, ambient temperature, height of tower and the surface of the collector.

Li et al. [13] have developed a thermal model of molten salt cavity receptor based on energy balance. Various factors, such as the surface of the receiver, the heat loss, the diameter of the tube, were analyzed to study the thermal performance of the cavity receiver.

Zhihao et al. [14] developed an HFLD software tool for designing heliostats field design and performance calculation based on energy balance. The ultimate goal of their work is to predict the transient behavior of thermodynamic parameters associated with external disturbances and change of operational inputs.

Ershu et al. [15] modeled a solar thermal plant (DAHAN) using the modular modeling method. The mathematical models of the heliostat field and the receiver system are developed. The thermal storage system and the conventional power plant are modeled using STAR-90. The simulated results show the dynamic evolution of the steam temperature, the steam pressure, the steam flow and the power generated.

Qiang et al. [16] modeled the collector and cavity receiver of the same plant (DAHAN) and the dynamic characteristics were studied under different perturbations based on the 'STAR-90' simulation platform.

Ferrière et al. [17], Yebra et al. [18] developed their own model of the receiver which corresponds respectively to the French tower plant "Themis" and the Spanish power station "CESA-I". Their model is based on the energy balance.

A study was proposed by Qiang et al. [19] to simulate the dynamic behavior of the solar cavity receiver under large and fast solar disturbances. Thermal losses were also calculated and analyzed under different wind conditions. In their results, suggestions were recommended to adjust the initial design.

Montes et al. [20] proposed a fluid flow arrangement to improve heat transfer in the active absorber surface of the receivers in the solar central cavity. The proposed design is consistent with the symmetry of the solar image on the surface of the absorber. Thus, the overall mass flow rate of the HTF is divided into as many circuits as quasi-symmetrical regions can be defined on the surface of the absorber. In this way, more uniform temperatures are reached at the outlet of all the circuits, which reduces the irreversibilities of the mixture.

Sahoo et al. [21] studied heat loss due to radiation and laminar natural convection in a trapezoidal cavity with eight absorber tubes for a linear Fresnel reflector solar thermal system (LFR) with uniformly heated tubes and adiabatic top wall. He observed that the dominant mode of cavity heat loss is radiation. They proposed using a selective coating on the tubes and cavity inside the wall to reduce overall losses. Although the dominant loss mode is radiation, natural convection losses are also important.

Wei et al. [22] developed a new computer code, based on a new method for designing the heliostat field configuration (HFLD) for a solar tower power plant. In this method, the boundaries of the field are constrained by the geometric opening of the receiver and by the efficiency factor.

Xu et al. [23] developed an energy and exergy analysis for the main subsystems of the solar power plant. They assessed the effect of DNI and concentration ratio on energy and exergy yields, as well as the effect of the concentration ratio on the surface temperature of the receiver and on the opening area of the receiver.

Ronan et al. [24] developed a mathematical model to evaluate the influence of system temperatures,

Copyright © 2021, Algerian Journal of Environmental Scien ce and Technology, All rights reserved

thermal conductance and receiver irradiance on optimal receiver temperature and solar / electrical efficiency of solar power plants and solar towers. Melted salts used as a working fluid, they found that the optimum value of the energy irradiation level of the receiver is about 200 kW / m2 for solar tower and solar trough systems. Hence, optimized receiver temperatures suggest the use of subcritical ranking cycles for solar power plants, except for super critical ranking cycles for tower solar power plants.

In this paper, genetic algorithms are proposed as a new approach to optimizing the present problematic whose constraints and objective functions are inspired by the energy balance calculation of the tower solar system (CSP).

II. Mathematical models

II.1. Principle of a solar tower plant operation

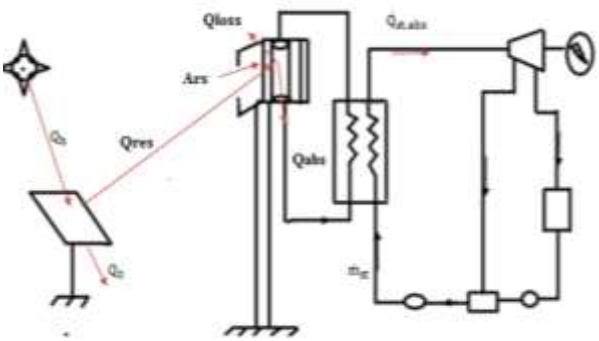

Figure 1. *Schema representing the different powers.*

In the incident power of the sun Q_h, one of its fraction will be transferred into the environment (lost) on the other hand the other Q_{rec} will be reflected towards the receiver (a cavity at the top of a tower) where there will be a heat transfer with the heat transfer fluid (molten salt). The receiver heat flow is made up of two components, the absorbed heat flow Q_{abs} and the waste heat flow Q_{loss}.

The heat flow Q_{abs} is absorbed by the heat transfer fluid which will be entirely transmitted to the exchanger in order to produce the water vapor which in turn drives the steam turbine to produce electricity

Table 1. *The principal characteristics of the tower solar concentration systems (CSP)*

characteristics	value	unit
location parameters of the area:		
- Direct Normal Irradiation DNI	800	W/ m^2
heliostat field:		
- Heliostat field surface	3.106	m^2
- Total surface of heliostat	2.105	m^2
- Overall efficiency of the heliostat field [6]	0.75	-
- Concentration factor [25]	5000	-
Receiver:		
- receiver surface	80	m^2
- receiver opening surface	20	m^2
- Inlet temperature of molten salt	290	°c
- Melted salt outlet temperature	565	°c
- View factor	0.25	-
- Tube diameter	0.019	m
- Thickness of tube	0.0016	m
- Emissivity	5	-
- Reflectivity	0.8	-
- Concentration factor	0.04	-
- Wind speed	5000	m/s
- Wall thickness of the receiver wall	5 0.4	m
Power block:		
- Water inlet temperature	239	°c
- Exit temperature of the water vapor	552	°c
- Ambient temperature	20	°c
- Net electricity power	$3{,}4.10^6$	w

II.2. Energy balance model

The analysis of each subsystem allows calculating the heat balance based on the principle of energy conservation.

The energy balance of a volume control is expressed as follows:

$$\dot{W}_{c.v.} = \sum_j \dot{Q}_j + \sum_{in} \dot{m}_{in}\, h_{in} - \sum_{ex} \dot{m}_{ex} h_{ex} \qquad (1)$$

where:

$\dot{W}_{c.v.}$: Work absorbed or delivered by the control volume.

$\dot{Q}_j$: Thermal energy absorbed or delivered by the system.

$\dot{m}_{in}$ and $\dot{m}_{ex}$: Inlet and outlet mass of the flow.

h_{in} and h_{ex} : Enthalpy at the entrance and the exit of the system.

II.2.1. Heliostat field model

The energy balance at the heliostat field is given by the following equation:

$$Q_h = Q_{rec} + Q_0 \qquad (2)$$

Or :

Copyright © 2021, Algerian Journal of Environmental Science and Technology, All rights reserved

Q_h : Incident solar energy

Q_{rec}: Energy transmitted to the receiver.

Q_0: Loss of energy in the environment which are the effects of losses of the heliostat field (cosine, shading, blocking, overflow, reflection and dispersion).

In practice, the overall efficiency of the heliostat field is given by :

$$\eta_h = \eta_{cos}.\eta_{omb}.\eta_{bloc}.\eta_{deb}.\eta_{ref}.\eta_{disp} \quad (3)$$

We assume in our study that $\eta_h = 75\%$ and that this η_h is defined as the ratio of the incident energy of the heliostat to the receiver (cavity) $\dot{Q}^*_{re}$ and the incident solar energy $\dot{Q}^*_h$.

so :

$$\eta_h = \frac{Q_{rec}}{Q_h} = \frac{Q_{rec}}{A_{ch}.q} \quad (4)$$

A_{ch}: Surface of the heliostats field.q: Direct normal irradiation (DNI).

or:

$$\frac{Q_{rec}}{A_{ch}.q.\eta_h} = \frac{(T_{rc}-T_a)A_f/Fr/c}{d_0/d_i/d_{ms}+d_0 ln(\frac{d_0}{d_i})/2/\lambda_{Tube}}$$

$$Q_{rec} = A_{ch}.q.\eta_h = \frac{(T_{rc}-T_a)A_f/Fr/c}{d_0/d_i/d_{ms}+d_0 ln(\frac{d_0}{d_i})/2/\lambda_{Tube}} \quad (5)$$

II.2.2. Central cavity receiver model

The efficiency of the central receiver ηre, is defined as being the ratio between the absorbed thermal energy Q_{abs} and the incident energy provided by the heliostats Q_{rec}. It is given by the following relation:

$$\eta_{rec} = \frac{Q_{abs}}{Q_{rec}} \quad (6)$$

The energy balance at the receiver is given by :

$$Q_{rec} = Q_{abs} + Q_{loss} \quad (7)$$

Such as:

$$Q_{abs} = \dot{m}_{st}(h_5 - h_4)$$

(8)

Q_{loss}: designates the energy losses in the receiver and represents the heat transfers by conduction, convection, radiation and reflection.

$$Q_{loss} = \frac{[(h_{air.fc.insi}(T_{rc}-T_a))+(0.81(T_{rc}-T_a)^{0.426}(T_{rc}-T_a)/Fr]}{A_f/C} + \left[\frac{\varepsilon_{avg}\sigma(T_{rc}^4-T_a^4)A_f}{C}\right] + [Q_{rc}.Fr.\rho] + [(T_{rc} - T_a)A_f/(\delta_{insu}/\lambda_{insu} + 1/h_{air0})Fr.C]$$

(9)

From where, Q_{rec} become:

$$Q_{rec} = \dot{m}_{st}(h_5 - h_4) + \frac{[(h_{air.fc.insi}(T_{rc}-T_a))+(0.81(T_{rc}-T_a)^{0.426}(T_{rc}-T_a)/Fr]}{A_f/C} + \left[\frac{\varepsilon_{avg}\sigma(T_{rc}^4-T_a^4)A_f}{C}\right] + [Q_{rc}.Fr.\rho] + [(T_{rc} - T_a)A_f/(\delta_{insu}/\lambda_{insu} + 1/h_{air0})Fr.C] \quad (10)$$

II.2.3. Steam generating subsystem model (SGS)

It is the essential element in this solar power station because it provides the connection between the receiver and the steam turbine.

Its principle is to transfer the energy acquired by the molten salt from the receiver to the water circulated in the steam turbine.

The energy balance of the (SGSS) is given by:

$$\dot{Q}_{re,abs} = \dot{m}_{ms}(h_{ms,b} - h_{ms,a}) = \dot{m}_{st}(h_{st,5} - h_{st,4}) \quad (11)$$

With:

$\dot{m}_{ms}$: The mass flow of molten salt, $\dot{m}_{st}$: The mass flow of steam.

II.3. Power block model

Hirn cycle with Reheating and racking:

In figure 2, part of the steam flow (x) from the first turbine body is diverted to a mixer operating at intermediate pressure. In this mixer, the withdrawn vapor is mixed with the liquid flow (1 -x) of the condenser.

The amount of vapor (1-x) that leaves the first body of the turbine is used to increase the temperature from the exchanger and returns to the second body of the turbine.

The vapor condenses on contact with the cold liquid from the condenser, which has the effect of preheating the liquid. The vapor stream withdrawn (y) is calculated so that the final temperature of the liquid is precisely the saturation temperature corresponding to the intermediate pressure.

At the output of the mixer, a saturated liquid is obtained at the intermediate pressure and at the intermediate temperature, which is then injected into the boiler. The total flow of steam is thus reconstituted.

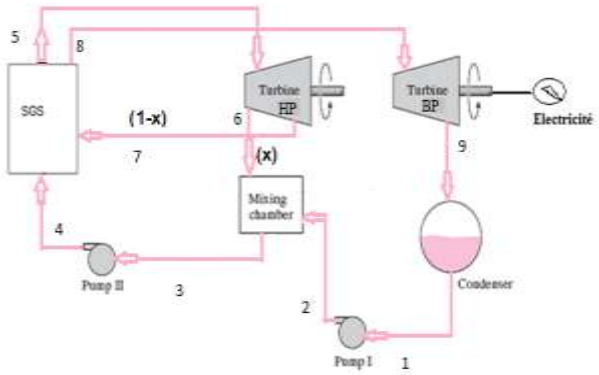

Figure 2. *Block diagram Hirn cycle with Reheating and racking.*

Copyright © 2021, Algerian Journal of Environmental Scien ce and Technology, All rights reserved

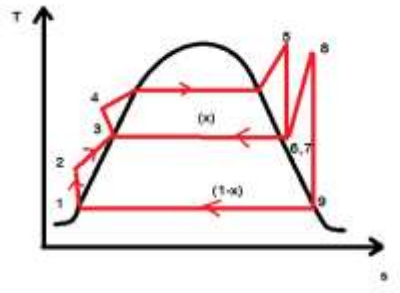

Figure 3. *Diagram (T-S) of Hirn cycle with Reheating and racking.*

The Hirn cycle consists of four transformations, Figure. 3:

• Transformation 1-2: Isentropic compression of the liquid just initially saturating, low pressure, in the pump1.

• Transformation 2-3: preliminary heating up to saturation and intermediate pressure.

• Transformation 3-4: Isentropic compression of the liquid just initially saturating, from medium pressure to high pressure in the pump2.

• Transformation 4-5: Isobaric (HP) heating-vaporization savings in the boiler to the superheated steam condition.

• Transformation 5-6: expansion in the low pressure turbine and, here a part of the steam stream from the first turbine body (x) is derived to a mixer operating at the intermediate pressure.

• Transformation 7-8: isobaric heating-vaporization for the amount (1-x) in the boiler to the superheated steam condition.

• Transformation 8-9: Relaxation of the amount (1-x) of the steam in the second body of the turbine high pressure (during this stage of the energy is provided as work outside the steam engine).

• Transformation 9-1: condensation of the quantity (1-x) at constant pressure in the condenser.

Hirn cycle efficiency with overheating and racking [26]:

$$\eta = \frac{h_5 - h_7 + h_8 - h_9}{h_5 - h_1 + h_8 - h_1} = 0.43 \qquad (12)$$

III. Effects of energy balance parameters on the performance of the solar system

In this section, the effects of the evolution of each element on the other of the energy chain is studied in order to better understand and to choose the constraints of the optimization problem of the solar system under study.

III.1. Variation of heliostat field surface as a function of DNI

Figure 4 presents the evolution of the area of the heliostats field as a function of the incident DNI:

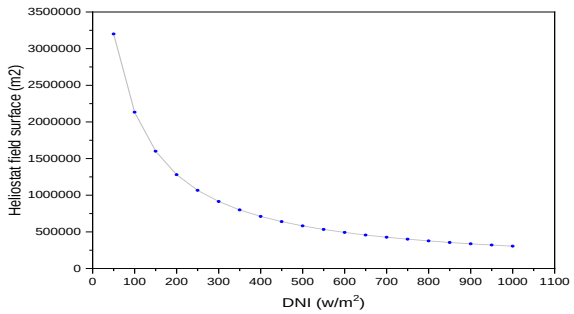

Figure 4. *Influence of heliostat field surface as a function of DNI.*

In figure 4, the increase in the DNI causes a decrease on the surface of the heliostat field, the relationship between the surface of the heliostat field and the DNI is inversely proportional. We find that the decrease of heliostats field surface from the value of 50 W / m^2.

III.2. Variation of the heliostat field efficiency according to the DNI

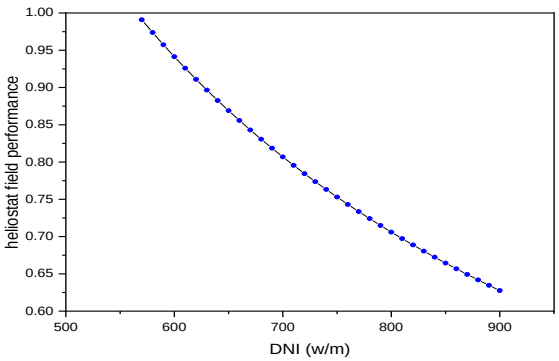

Figure 5. *Efficiency of the heliostat field as a function of the DNI.*

In figure5, the increase of DNI accompanies the reduction of the heliostat field performance and that due to the effects of the heliostat field losses.

III.3. Variation of incident flux, flux lost and flux absorbed as a function of receiver temperature

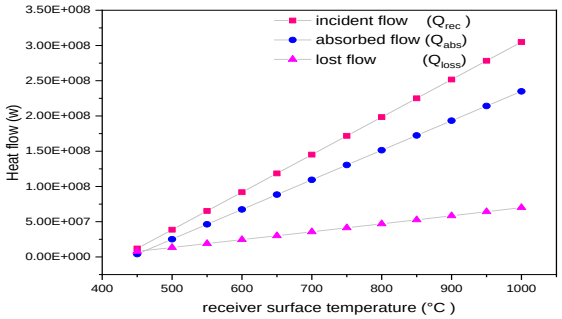

Figure 6. *Influence of Q_{rec} , Q_{loss} and Q_{abs} as a function of T_{rec}.*

Copyright © 2021, Algerian Journal of Environmental Science and Technology, All rights reserved

Figure. 6, shows the effects of the receiver surface temperature on the absorbed heat flow (Q_{abs}), the incident heat flow (Q_{rec}) and the loss of heat flow (Q_{loss}) of the receiver.
The increase in flows follow the form of an affine function of positive tangent and this tangent increases rapidly for the flow of the receiver then the flow absorbed and a decrease for the flow of losses.

III.4. Variation of incident flux according to the

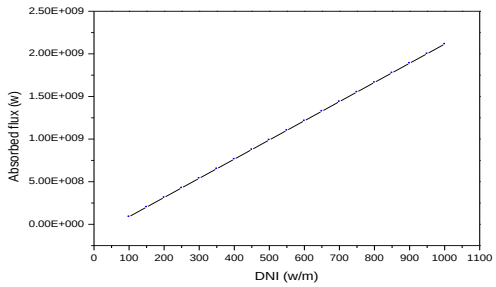

Figure 7. *Influence of incident flows according to the DNI.*

In the figure.7, We observe that the increase of absorbed flux related with the increase the DNI.

III.5. Variation of the receiver efficiency as a function of its temperature

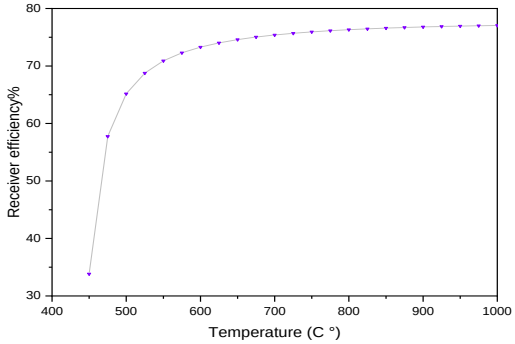

Figure 8. *The receiver according to T_{rec}.*

Figure 8 shows the evolution of the receiver's efficiency as a function of its temperature. For a temperature below 700 °c, growth rate accelerates rapidly in the receiver, because there is an increase in energy absorbed by the surface of the receiver.
It can be also noted that at a temperature of 700 ° C efficiency reaches a threshold value (0.78) and almost constant until the end.

III.6. Variation of water steam flow as a function of receiver temperature and receiver opening

The evolution of the mass flow rate of the steam generated as a function of the temperature of the receiver surface for different openings of the cavity is shown in figure.9.

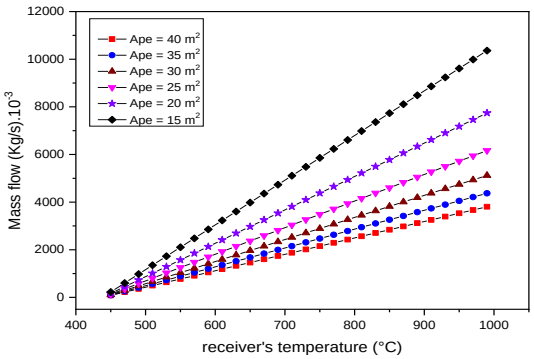

Figure 9*. The evolution of the mass flow rate as a function temperature with several openings.*

In figure 9, it can be seen that with the increase in the temperature of the receiver. the flow increases linearly and the openings of the cavity decrease and move away in a regular and progressive manner and this results from the reduction of the losses.

III.7. Variation of water steam flow as a function of the receiver temperature and the receiver surface

The evolution of the molten salt mass flow generated based on the temperature of the surface of the receiver for different values of the surface of the opening of the cavity.
The results are shown in Figure. 10.

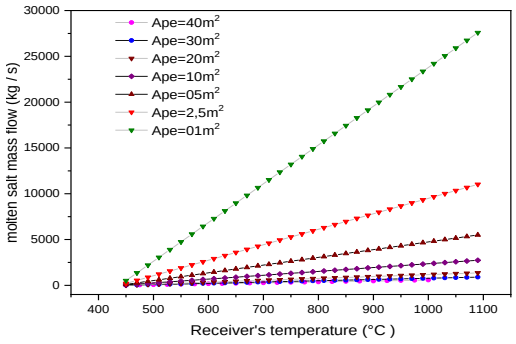

Figure 10. *The evolution of the mass flow rate as a function temperature with several surfaces.*

In figure.10, for large openings, the evolution of the flow as a function of the temperature is very slow because of the large heat losses, which requires considerable energy to melt the salt. On the other hand, for small openings below 10 m2, the flow rate increases considerably, which explains a reduction in heat loss (greenhouse effect phenomenon inside the cavity) and an acceleration of slope.

Copyright © 2021, Algerian Journal of Environmental Scien ce and Technology, All rights reserved

IV. Simulation Results and comments

Two optimization problems may be studied: maximization of Q_{rec} (equation 10) and minimization of Q_{loss} (equation 9).

IV.1. Optimization first problem

A. Constraints:

$10000 \leq Af \leq 200000$
$450 \leq Trc \leq 1000$
$290 \leq Tms \leq 565$
$1 \leq Ape \leq 40$
$40 \leq Arc \leq 300$
$0.01 \leq di \leq 0.02$
$0.001 \leq Epss \leq 0.01$
$16 \leq \lambda_{tube} \leq 1000$

B. Objective function:

Maximizing (Equation 10)

IV.2. Optimization second problem

A. Constraints:

$10000 \leq Af \leq 200000$
$450 \leq Trc \leq 1000$
$290 \leq Tms \leq 565$
$1 \leq Ape \leq 40$
$40 \leq Arc \leq 300$
$0.01 \leq di \leq 0.02$
$0.001 \leq Epss \leq 0.01$
$16 \leq \lambda_{tube} \leq 50$

B. Objective function:

Minimizing (Equation 9)

Genetic algorithms are used for the simulation of equations 9 and 10.

The genetic algorithms (AGs) [27]: are stochastic optimization algorithms based on the mechanisms of natural selection and genetics. Their operation is extremely simple. We start with a population of initial potential solutions arbitrarily chosen. Their relative fitness (fitness) is evaluated. On the basis of this performance we create a new population of potential solutions using simple evolutionary operators: selection, crossing and mutation. This cycle is repeated until the completion of a solution.

Table.2 and figure 11, presents the optimal value of each parameter regarding the first and second problems successively and their comparison:

Table 2. *Comparison of the optimal values of each study.*

Studies / Parameters	Chao Xu[7]	S.Benammar [6]	Present work
Receiver temperature T_{rc}	543.3647	559.5522	753.0534
Total surface of heliostat A_f	9500	4748	10846
Receiver opening surface A_{pe}	12.7895	1.199	16.4792
Receiver surface A_{rc}	57.2020	10.9995	55.0468
Internal diameter di	0.0195	0.0192	0.01
Thickness of tube ep	0.00168	0.0017	0.0067
Conductivity λ_{tube}	19.9451	23.9266	25.1984
Average temperature of molten salt T_{ms}	542.7249	557.5038	554.8457
Q_{rec}	9.5477E+03	9.8886E+03	8.3188E+06
Q_{abs}	7.5933E+03	7.8354E+03	8.3171E+06
Q_{loss}	1.9544E+03	2.0532E+03	0.0017E+06

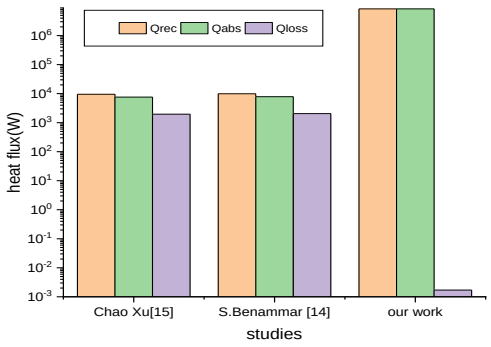

Figure 11. *Explanatory histogram of the results (heat flux) of the current work and its comparison with previous works.*

Comparison of the absorbed and lost receiver flux found by the results of Chao Xu [7], S. Benammar [6] and the present work . It is found that the performance of the receiver in this work is much better compared to that of antecedent works.

Copyright © 2021, Algerian Journal of Environmental Science and Technology, All rights reserved

In figures 12, 13 and 14, it is clear that the performance parameters of the CSP system found in this paper such as the heliostat surface, the heat flows and the efficiency of the receiver have the same behavior of evolution versus to the work of S. Benammar, despite the difference between The mathematical models and the numerical tools used in the two works.

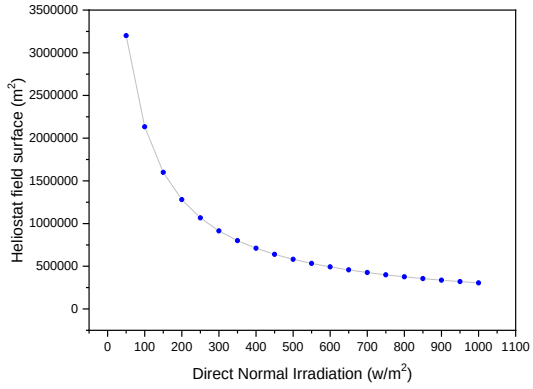

a

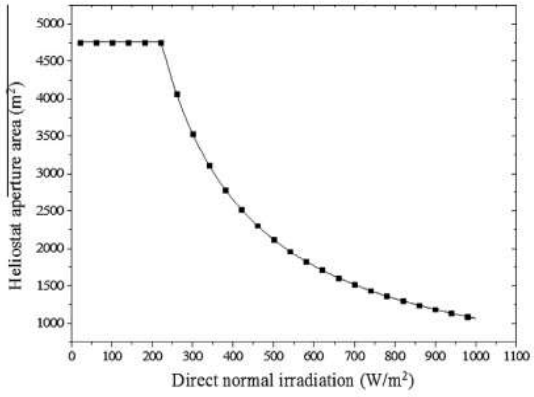

b

Figure 12. *Influence of the heliostat field surface as a function of DNI. a: Our work and b: S.Benammar [6].*

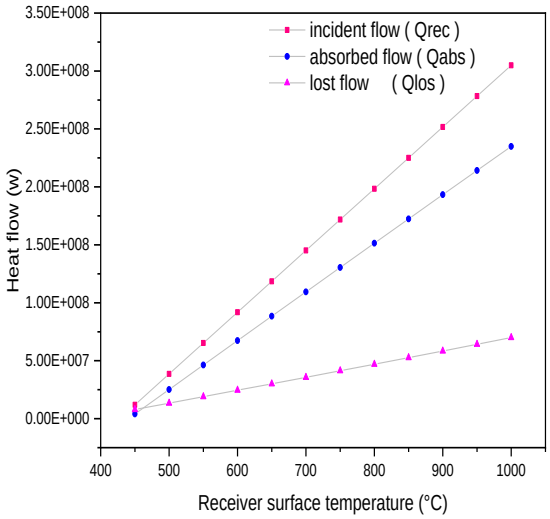

a

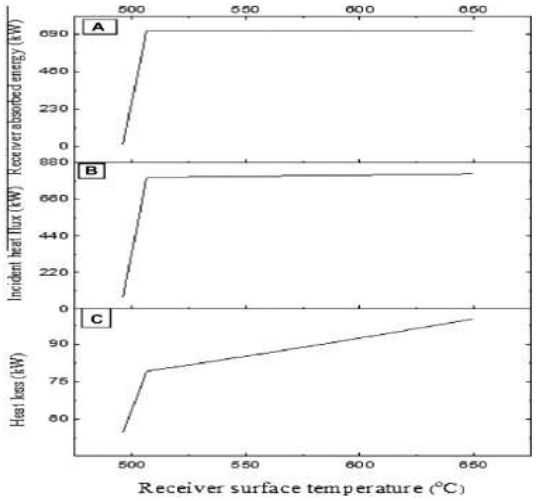

b

Figure 13.*Influence of the flows: incident, lost and absorbed as function of the receiver's temperature a: Our work and b: S.Benammar **[6]**.*

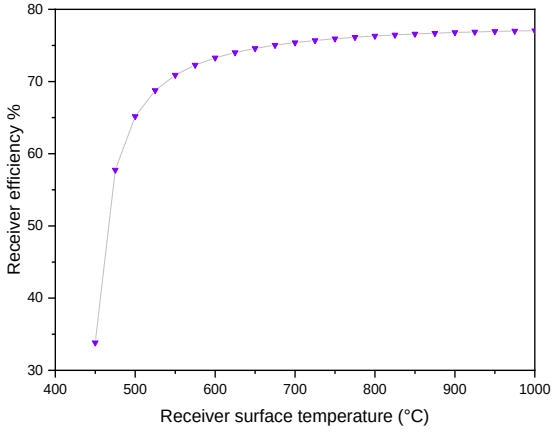

a

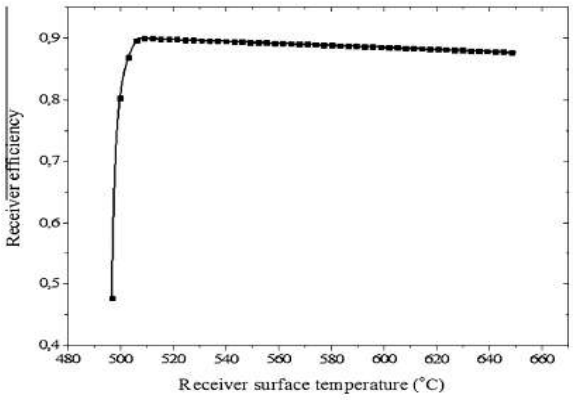

b

Figure 14*. the efficiency of the receiver as function on its temperature. a: Our work and b: S.Benammar **[6]**.*

Copyright © 2021, Algerian Journal of Environmental Scien ce and Technology, All rights reserved

V. Conclusion

In this paper, a non-linear mathematical model based on the analysis of the energy balance has been developed to optimize the performance of thermodynamic solar tower systems (CSP). Genetic algorithms are thus proposed as a new approach for solving the complex optimization problem whose constraints and objective functions are obtained from the energy balance.

The obtained simulation results play a very important role in the choice of a quasi-real design and represent an appropriate guide for the manufacturer for the good dimensioning of the components of the receiver thus the choice of its materials (di, ep, λtube, insulation).

The obtained simulation results lead to the following conclusion points:

- ✓ The choice of a quasi-real design with an appropriate guide for the manufacturer for the correct sizing of the receiver components and the choice of its materials (di, ep, λtube, insulation).
- ✓ Optimization of the dimensioning parameters of the receiver (Trec ,, Arc, Ape, di, ep, λtube,) which in turn allows the maximization of the absorbed heat flow Qabs and the minimization of losses of the heat flow Qloss in the receiver .
- ✓ To have an optimal incident heat flow received Qrec which is the result of the DNI influence on the heliostat field with the minimization of its loss effects.
- ✓ The obtained effeciency of the Qabs / Qrec receptor is much better compared to that of the literature.

VI. References

1. Mohammad, H. A. ;Mahyar.G. ;Milad,S. ;Mohammad,A.N.;Ravinder, K. ; Abbas,N.;Tingzhen,M. Solar power technology for electricity generation: A critical, Energy Sci Eng. (2018); 6: 340–361.
2. Abdelkader, R. ; Djamel, B. ; Rahmani, K. ; Awf,A. ; Justo, G.S.C. ; Khaled. M. Solar Tower Power Plants of Molten Salt
External Receivers in Algeria: Analysis of Direct Normal Irradiation on Performance, Appl. Sci.(2018), 8, 1221.
3. Kun,W. **;** Ya-Ling, H. Thermodynamic analysis and optimization of a molten salt solar power tower integrated with a recompression supercritical CO2 Brayton cycle based on integrated modeling. Energy Conversion and Management (2017); 135 **:**336-350.
4. Zhirong,L. ; Amir,F. Thermal analysis of a heat pipe solar central receiver for concentrated solar power tower. Applied Thermal Engineering.(2016).04.043.doi: http://dx.doi. org/ 10. 1016/j.applthermaleng.
5. Tehrani,S. S. M. ; Robert,A. T. Off- design simulation and performance of molten salt cavity receivers in solar tower plants under realistic operational modes and control strategies. Applied Energy journal homepage: www. elsevier. com/ locate/ apenergy.
6. Benammar, S. Contribution to the modeling and simulation of solar power tower plants using energy analysis. Energy Conversion and Management(2013).www.elsevier.com/locate/ enconman
7. Chao, X. Energy and exergy analysis of solar power tower plants, Applied Thermal Engineering. (2011) . www. elsevier. com/ locate/apthermeng
8. Zhihao, Y.; Zhifeng W.; Zhenwu, L.; Xiudong,W. Modeling and simulation of the pioneer 1MW solar thermal central receiver system in China. Renewable Energy.(2009); 34:2437-46.
9. Prakash, M. ; Kedare, S. B. ; & Nayak, J. K.Investigations on heat losses from a solar cavity receiver, Solar Energy.(2009); 83: 157-170.
10. Montes, M.J. ; Abánades, A. ; Martínez-Val ,J.M.Performance of a direct steam generation solar thermal power plant for electricity production as a function of the solar multiple.Solar Energy. (2009); 83:679-689.
11. Montes, M.J. ; Abánades, A. ; Martínez-Val,J.M. ; Valdés, M. Solar multiple optimization for a solar-only thermal power plant, using oil as heat transfer fluid in the parabolic trough collectors, Solar Energy. (2009); 83: 2165-76.
12. Larbi, S. ; Bouhdjar, A. ; Chergui, T.Performance analysis of a solar chimney power plant in the southwestern region of Algeria, Renewable and Sustainable Energy Reviews. (2010); 14: 470-477.
13. Li, X. ; Kong, W. ; Wang, Z. ; Chang, C. ; Bai, F. Thermal model and thermodynamic performance of molten salt cavity receiver, Renewable Energy (2010); 35: 981-988.
14. Yao, Z. ; Wang, Z. ; Lu, Z. ; Wei, X.Modeling and simulation of the pioneer 1MW solar thermal central receiver system in China. Renew Energy(2009); 34:2437-46.
15. Xu, E . ; Yu, Q. ; Wang, Z. ; Yang, C. Modeling and simulation of 1 MW DAHAN solar thermal power tower plant. Renew Energy (2011); 36:848–857.
16. Yu, Q . ; Wang, Z. ; Xu, E. Simulation and analysis of the central cavity receiver's performance of solar thermal power tower plant. Solar Energy (2012); 86:164–74.
17. Ferriere, A.; Bonduelle, B. ; Amouroux, M. Development of an optimal control strategy for the thémis solar plant: Part 1 – Themis transient model. Trans ASME (1989); 111:298–304.
18. Yebra, L.J .; Berenguel, M.; Dormido, S.; Romero, M. Modeling and simulation of central receiver solar thermal power plants. In: Proceedings of the 44th IEEE conference,Spain; (2005).
19. Yu, Q.; Wang, Z .; Xu, E .; Li, X.; Guo, Minghuan. Modeling and dynamic simulation of the collector and receiver system of 1 MWe DAHAN solar thermal power tower plant. Renew Energy (2012); 43:18–29.
20. Montes, MJ .; Rovira, A .; Martínez-Val, JM .; Ramos, A. Proposal of a fluid flow layout to improve the heat transfer in the active absorber surface of solar central cavity receivers. Appl Therm Eng (2012); 35:220–32.
21. Sahoo, S. S .; Singh, S .; Banerjee, R. Analysis of heat losses from a trapezoidal cavity used for Linear Fresnel Reflector system. Solar Energy (2012);86:1313–22.

Copyright © 2021, Algerian Journal of Environmental Science and Technology, All rights reserved

22. Wei, X .; Lu, Z .; Wang, Z .; Yu, W .; Zhang, H.; Yao, Z. A new method for the design of the heliostat field layout for solar tower power plant. Renew Energy (2010); 35:1970–5.
23. Xu, C .; Wang, Z .; Xin, L .; Sun, F. Energy and exergy analysis of solar power tower plants. Appl Therm Eng (2011); 31:3904–3913.
24. McGovern, R. K .; Smith, W. J. Optimal Concentration and temperatures of solar thermal power plants. Energy Convers Manage (2012); 60:226–32.
25. ''Manuel Romero-Alvarez and Eduardo Zarza'','Handbook of Energy Efficiency and Renewable Energy', Plataforma Solar de Almeria-CIEMAT, by Taylor & Francis Group, LLC (2007).
26. Extrait de "Systèmes Energétiques, tome 2", Presses de l'Ecole des Mines de Paris (2005).
27. ''Thomas Vallée'' et ''Murat Yıldızoglu'' ' Présentation des algorithmes génétiques et de leurs applications en économie', Université de Nantes, LEA-CIL. septembre (2001).

Nomenclature

A	Area	m^2
C	concentration ratio	/
d	Diameter	m
Fr	View factor	/
h	Enthalpy , Heat Transfer Coefficient	J. kg^{-1} , $W(m^2K)^{-1}$
c_p	specific heat,	$J.(kg\ K)^{-1}$
$\dot{m}$	mass flow rate	kg s^{-1}
$\dot{Q}$	heat transferred	W
$\dot{q}$	heat flux	W m^{-2}
s	entropy	J. k^{-1}
T	Temperature	K
$\dot{W}$	work or power	W

Greek

δ	Thickness	m
$\boldsymbol{\lambda}$	Thermal conductivity	$W(m.k)^{-1}$
σ	Stefan Boltzmann constant	$5{,}67.10^{-8} W(m^2k^4)^{-1}$
ε	receiver surface emissivity	/
η	Efficiency	/
ρ	Density	$kg.m^{-3}$

superscripts

$*$	associated to solar rays

Subscripts

0	Reference
abs	Absorbed
avg	Average
a	at the inlet
b	at the outlet
cond	Conduction
con	convection
CSP	concentrated solar power
C.V	Control volume
em	Emissive
ex	Exit
fc	Forced convection
h	heliostat
HTF	heat transfer fluid
in	inlet
i	inner
insi	inner side of receiver
insu	insulation
ms	molten salt
nc	natural convection
o	outer
p	pump
pc	power cycle
rec	receiver
ref	reflective
SGS	steam generation subsystem
st	steam
STPP	solar tower power plants
Loss	total loss
Sur	surface
SPT	solar power tower

Please cite this Article as :
Rouibah,A; Benazzouz,D; Rahmani,K; Benmessaoud,T.Performance analysis and optimization of molten a salt cavity receiver in solar power pllants. ***Algerian J. Env. Sc. Technology***, ***7*:2 (2021) 1870-1879**

Copyright © 2021, Algerian Journal of Environmental Scien ce and Technology, All rights reserved